VOL. 12, NO. 21, NOVEMBER 2017 ISSN 1819-6608
ARPN Journal of Engineering and Applied Sciences

www.arpnjournals.com

OPTIMAL SPEED CONTROL BASED ON ADAPTIVE SECOND ORDER SLIDING MODE AND MODIFIED HSC MPPT ALGORITHM FOR WIND TURBINES

Morad Hafiane, Jalal Sabor and Mohammed Taleb
CP2S team / LSMI laboratory -ENSAM-Meknes, Morocco
E-Mail: morad.hafiane@gmail.com

ABSTRACT

Accurate control of the wind turbine at its optimal rotational speed for a given wind speed is required to extract maximum power from the wind turbine generator system in the absence of aerodynamic pitch control. Due to inherent wind turbine nonlinearities and unpredictable wind speed fluctuations, precise control is a difficult task to undertake. This paper presents a command strategy of doubly fed induction generator (DFIG) which based on a maximum power point tracking (MPPT) algorithm with a modified Hill Climb Searching (HCS) and a sliding mode controller with adaptive twisting algorithm in order to achieve accurate tracking under the wind turbine's nonlinear dynamics and fast wind changes. Simulation results for different situations highlight the performance of the proposed strategy under various wind speed operating conditions.

Keywords: wind turbine (WT), hill climb searching (HSC), doubly fed induction generator (DFIG), high order sliding mode (HOSM), adaptive twisting (AT).

1. INTRODUCTION

In the last decade, alternative energy sources such as renewable energies have received a thorough attention and have been considered as a way of fighting climate change. Among renewable energies, wind turbine has become the world's fastest growing energy generator.

Variable speed wind turbines are widely used in many high performance applications and offer several advantages with respect to their fixed speed counterpart, such as maximum power extraction from the wind and reduced power electronics requirements and costs. Thus, a variable speed generator achieves optimal energy generation by adjusting its rotational speed to track wind speed. However, wind turbine dynamics is highly nonlinear and wind speed is continuously variable and unpredictable. The conflicting requirements between the nature of wind and optimal energy generation make the wind turbine control task a challenging research problem. Typical challenges include varying operating conditions, high nonlinearities, and external disturbances. This raises the urgency to consider alternative control approaches for efficient power generation to keep up with the increasingly energy demand requirements.

Several generator types are used in wind turbines, such as Doubly Fed Induction Generators [1],[2] and permanent magnet synchronous generators[3]. The permanent magnet synchronous generators require high power converters to allow the wind turbine speed variation, and also to permit its connection to stable grids under various wind speeds, this requires an over sizing of the power converter which should be at least the same power as the wind turbine generator, therefore increases the overall cost [1], in addition to the high generator cost. The use of DFIGs reduces considerably the cost of the WT systems [1]. Indeed, the generator speed variation is performed by placing a rotor side inverter, whose power represents only 25% of the wind turbine generator power [1].

Under various wind speed, the wind turbine operates, in four regions (Figure-1) as follow [4]:

The first and the fourth region, in which the wind turbine should be stopped and disconnected from the grid to avoid that it be driven by the grid and also to prevent mechanical system damages respectively. A second region is a linear area which the power depends on the wind speed, and a maximum power point tracking (MPPT) system is required to extract the maximum power from the wind, and finally the third region, that corresponds to the maximal turbine speed, in which the power is kept constant by adjusting blades angle (pitch control) to avoid mechanical damages.

In the second area, the optimal power can be obtained, by adjusting the generator speed to follow its optimal value generated by an MPPT system, this latter and according to the wind change, wind turbine specifications, and operating generator speed, generates an optimal set point to the inverter in rotor side and then controls the speed generator. The maximum power can only get provided by variable speed turbines.

Regarding the MPPT algorithms, there are two main categories [4]: The Direct Power Control (DPC), in which the MPPT algorithm acts directly on the output power [].And the Indirect Power Control (IPC) in which the MPPT algorithm controls the output power by acting on the mechanical input power.

In the IPC category, we find the Tip Speed Ratio (TSR) MPPT algorithm [4], [5], that works to keep up the TSR to an optimum value, which corresponds to a maximum input power by adjusting the generator speed [4],[5]. This algorithm is known for its simplicity. However, it requires a permanent measure of wind speed [4].

A second algorithm in same category is the Optimal Torque OT [4], [5], [7] MPPT algorithm, in which the generator is controlled to obtain an optimal torque at a given speed. Hens the optimal power is obtained. And finally, the power signal feedback (PSF) MPPT algorithm [4], [6], [7], in which the speed generator is controlled to obtain an optimal power based on the optimal curve. The OT and the PSF don't need anemometers. However, they require the parameters of specific wind turbine [4], [5], [6], [7].

The first algorithm considered under DPC is the hill climbing search (HCS) MPPT algorithm which known as perturb and observe (P&O) [4],[7],this latter is a sensorless algorithm [7], and it's widely employed in many WT and photovoltaic (PV) applications, because of its flexibility and simplicity. This algorithm is based on perturbing the speed generator with a fixed step size [7] then measuring its corresponding output power until reaching the maximal power point (MPP). However, and in a fast wind change the algorithm may lose the perturbation direction when the change in power is not due to the perturbation but due to the change in the wind speed [4], another problem with HCS occurred when choosing a large fixed step for the perturbation, this causes the oscillations around the MPP [4] which will never be reached, also choosing a small step size perturbation reduces the convergence time [4]. To overcome these drawbacks, as detailed in section II, a novel HCS modified algorithm has been introduced in [8] to resolve the perturbation direction and step size problems.

Another DPC algorithm was proposed in [4], [12], it's the incremental conductance (INC) algorithm, which is also sensorless algorithm, and doesn't require turbine specifications [4], [12]. In this algorithm the output power is considered as a DC link voltage (V_{dc}) [4], [12], [13], [14], and it's based on changing the V_{dc} with a fixed step until getting a maximal output power. However, the step size can generate oscillations around the MPP. In [4], [15], [16] a modified INC has been proposed, which is based on a variable step size to avoid the encountered problems.

At the end, the optimal relation based (ORB) algorithm, it's also sensorless algorithm, and it's based on a pre-obtained system curve [4], [17]. In this algorithm the MPP can be tracked by working on the optimal current curve at all times [4], [18]. And the current command in a specific wind speed should not exceed the maximum current curve [4].

To overcome the drawbacks of these algorithms, a hybridization of two or more algorithms may be applied [4], [18].

These algorithms described above do not represent all MPPT algorithms, although there are other algorithms such as fuzzy logic algorithms [4], [19], neural network algorithms [4], [20], [21], adaptive MPPT algorithms, and multi-variable P &O algorithms [4], [22]. These can act on the input power or the output power. However, they are a bit complicated, and require too much calculation. These are surmounted with the development in computing units.

The efficiency and the precision of these MPPT algorithms depend strongly on the characteristics of the wind turbine. Indeed, the significant inertia of the turbine and the time constants presented in the generator components influence the accuracy and the convergence time of these MPPT algorithms.

For this purpose, and especially for DFIGs, the conventional control such as PID controllers reduces the efficiency of the MPPT algorithms and especially in a fast wind change, as detailed in section V.

For DFIG, researchers attempted various control techniques and several solutions have been proposed including classical and robust control laws, such as vector and sliding mode control. The field-oriented vector control technique [23] is used for its simplicity. However, faster torque dynamic response is achieved with Direct Torque Control (DTC) [24] at the expense of current distortion, and torque ripple. These negative effects have been addressed using predictive DTC in [25] and a hybrid PWM technique in [26]. On the other hand, a sliding mode speed controller is proposed in [27]. However, robustness to parameter variations and uncertain load disturbance is obtained only when sliding mode truly occurs.

On another aspect, tools of computational intelligence, such as artificial neural networks (ANNs), have been credited in various applications as powerful tools capable of providing robust approximation for systems that may be subjected to structured and unstructured uncertainties [28]This has led to the recent advances in the area of intelligent control [29], [30]. Various neural network models have been applied to control the speed of doubly fed induction generators [31], [32], providing an alternative to conventional control techniques. Despite the success witnessed by ANN-based control systems, they face a significant complexity in their stability analysis.

As a robust control for DFIG, we find the sliding mode control theory, which was proposed by Utkin in 1977 [33]. Thereafter, the theoretical works and its applications were developed. Since the robustness is the best advantage of a sliding mode control, it has been widely employed to control nonlinear systems that have model uncertainty and external disturbances [31].

The application of the sliding mode theory began with the first order sliding mode controller, which used to control many nonlinear systems; this presents the advantage of robustness. However, it generates the chattering phenomenon, which represents high frequency oscillations around the operating set point (caused by a discontinued control law).

To reduce the chattering phenomenon, in [31] the authors have proposed, to change the control law expression with some continuous functions in order to avoid its high frequency switching.

So as to reduce this phenomenon, in [32] the author has proposed the super twisting algorithm (for High-order sliding mode), but it can only be applied to uncertain nonlinear systems featuring the relative degree one of the sliding variable (the relative degree is the number of time

which the sliding surface should be derived to get the control variable).

For the systems featuring the relative degree two of the sliding variable, the author has proposed the twisting algorithm [35] [36].

The application of the sliding mode algorithm to control a doubly fed induction generator (DFIG) is used to improve wind turbine generator efficiency at different wind operating conditions. In [37] the authors have introduced the first order sliding mode algorithm to control the DFIG. However, the chattering phenomenon remains the main problem.

In [38] and [39], the authors have introduced the high-order sliding mode using the super twisting and twisting algorithm to control the DFIG, in order to reduce the chattering phenomenon. But the problem to define the optimal parameters of these algorithms remains unsolved, and the authors have proposed some sufficient large values of these parameters.

In [40], [41], [42], [43], [44] new strategies to control DFIG based on adaptive parameters of the super-twisting and the twisting algorithm respectively, as detailed in section IV, have been introduced. The idea is based on increasing or decreasing the value of the algorithm parameters when it's required.

In this paper a new control strategy of a DFIG, which regroups an MPPT algorithm with a robust controller, based on high order sliding mode (HOSM), considering the significant advantages of each one. At the end a comparison study with a conventional control to show the interest and the effectiveness of the proposed strategy has been performed.

The rest of the paper is organized as follows: section II outlines the wind turbine dynamic model. The MPPT algorithm is detailed in section III. In section IV, the HOSM controller design. Simulation results are reported and discussed in section V. We conclude with some remarks.

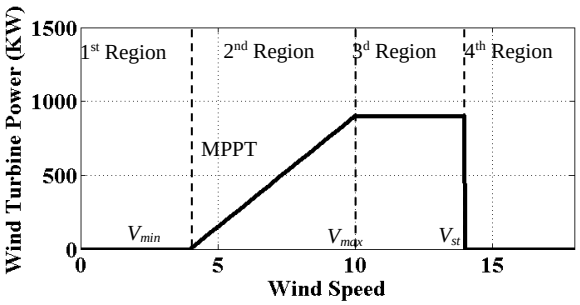

Figure-1. Wind turbine speed regions.

2. WIND TURBINE DYNAMICS

A. Wind dynamics

The dynamic equation of the power produced by a wind turbine [45], [46] is:

$$P = \frac{1}{2} c_p(\lambda, \beta) \rho \Pi R^2 v^3 \quad (1)$$

Where ρ is the air density, R is the turbine radius and v is the wind speed. Cp(λ,β) is the power coefficient, which represents the ratio between the blade tip speed and the wind speed as it's shown in Figure-2. $C_p(\lambda,\beta)$ is given by the equation [47],[48] below:

$$C_p(\lambda, \beta) = (0.44 - 0.0167\beta) \sin\left(\frac{\pi(\lambda - 3)}{(15 - 0.3\beta)}\right) - 0.00184(\lambda - 3)\beta \quad (2a)$$

Where, $\lambda = \frac{\Omega t.R}{v}$ (2b)

AndΩt is the wind turbine speed.

β : Turbine blades orientation angle

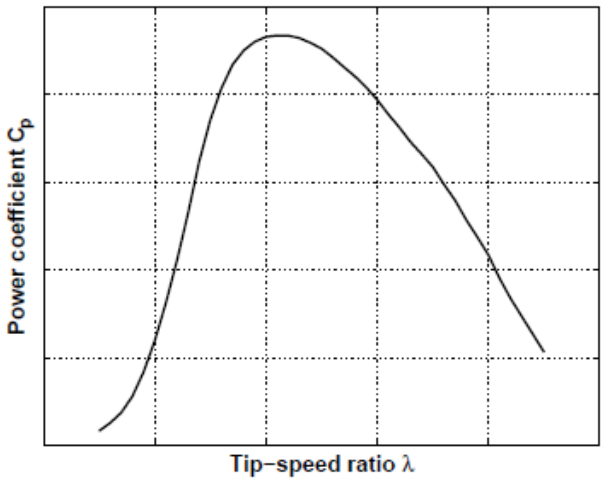

Figure-2. Power coefficient curve Cp(λ) versus tip speed ratio (TSR) λ, with β=0°.

B. Mechanical dynamics

The mechanical system equation can be expressed by:

$$J\frac{d\Omega}{dt} = C_t - C_{em} - C_f \quad (3)$$

Where,

J : generator and turbine Inertia
C_t : mechanical torque
C_{em} : electromechanical torque
C_f : friction torque.
Ω : angular generator speed.

C. Electrical dynamics

The DFIG dynamic mathematical model in the d-q axes rotating reference frame can be described by the following equations [51]:

$$v_{ds} = Rs.i_{ds} + \frac{d\phi_{ds}}{dt} - \omega s\phi_{qs} \quad (4a)$$

$$v_{qs} = Rs.i_{qs} + \frac{d\phi_{qs}}{dt} + \omega s\phi_{ds} \quad (4b)$$

$$v_{dr} = Rr.i_{dr} + \frac{d\phi_{dr}}{dt} - \omega r\phi_{qr} \text{(4c)}$$

$$v_{qr} = Rr.i_{qr} + \frac{d\phi_{qr}}{dt} + \omega r\phi_{dr} \text{(4d)}$$

With,

$$\phi_{ds} = Ls.i_{ds} + L_m.i_{dr} \quad (5a)$$

$$\phi_{qs} = Ls.i_{qs} + L_m.i_{qr} \quad (5b)$$

$$\phi_{dr} = Lr.i_{dr} + L_m.i_{ds} \quad (5c)$$

$$\phi_{qr} = Lr.i_{qr} + L_m.i_{qs} \quad (5d)$$

Where,

v_{ds}, v_{qs}	stator voltage in *d-q* axes
v_{dr}, v_{qr}	rotor voltage in *d-q* axes
i_{ds}, i_{qs}	stator current in *d-q* axes
i_{dr}, i_{qr}	rotor current in *d-q* axes
φ_{ds}, φ_{qs}	stator flux linkage in *d-q* axes
φ_{dr}, φ_{qr}	rotor flux linkage in *d-q* axes
R_s, R_r	stator and rotor resistance
L_r	rotor inductance
L_m	magnetizing (mutual) inductance
ω_s, ω_r	stator and rotor speed

The stator speed and electromechanical torque are described as,

$$\omega_s = \omega_r + P\Omega \quad (6a)$$

$$C_{em} = P(\phi_{ds}.i_{qs} + \phi_{qs}.i_{ds}) \quad (6b)$$

Where, P is the pole pair number. The active and reactive power are expressed as,

$$P_s = v_{ds}i_{ds} + v_{qs}i_{qs} \quad (7a)$$

$$P_r = v_{dr}i_{dr} + v_{qr}i_{qr} \quad (7b)$$

$$Q_s = -v_{ds}i_{qs} + v_{qs}i_{ds} \quad (7c)$$

$$Q_r = v_{dr}i_{qr} + v_{qr}i_{dr} \quad (7d)$$

The DFIGs are widely used in many industrial applications such as wind turbines and electric vehicles thanks to their high-performance and low cost [49]. However, these systems are driven by complex dynamics. To reduce this complexity, the generator's flux and torque are controlled separately. For that, a decoupling is achieved using a coordinate transformation, which is called field-oriented control (FOC) technique. Although this complexity reduction, their efficient operation is still limited by numerous challenges such as varying operating conditions, structured and unstructured dynamical uncertainties, and external disturbances. Therefore, DFIG flux is expressed as,

$$\phi_{ds} = \phi_s \quad (8a)$$

$$\phi_{qs} = 0 \quad (8b)$$

Which yields from (5a) and (5b)?

$$i_{ds} = \frac{\phi_s}{L_s} - \frac{L_m}{L_s}i_{dr} \quad (9a)$$

$$i_{qs} = \frac{L_m}{L_s}i_{qr} \quad (9b)$$

Therefore, the electromechanical torque (6b) is written as,

$$C_{em} = -P\frac{L_m}{L_s}\phi_s i_{qr} \quad (10)$$

Stator resistance is usually neglected for large machines and flux $\phi_s$is taken to be constant. Therefore, Formulation (4a) and (4b) can be written as,

$$v_{ds} = 0 \quad (11a)$$

$$v_{qs} = v_s = \omega_s\phi_s \quad (11b)$$

Substituting (9a) and (9b) in (5c) and (5d) yields,

$$\phi_{dr} = \frac{L_m}{L_s}\phi_s + \sigma Lr.i_{dr} \quad (12a)$$

$$\phi_{qr} = \sigma Lr.i_{qr} \quad (12b)$$

Where,

$$\sigma = 1 - \frac{L^2m}{L_sL_r} \quad (12c)$$

Substituting $\Phi_{dr}$and Φ_{qr} from (12) into (4c) and (4d) leads to,

$$v_{dr} = R_r.i_{dr} + \sigma Lr\frac{di_{dr}}{dt} - \omega_r\sigma Lr.i_{qr} \quad (13a)$$

$$v_{qr} = R_r.i_{qr} + \sigma Lr\frac{di_{qr}}{dt} + \omega_r.\sigma Lr.i_{dr} + g\omega_r \text{(13b)}$$

Where, $g = \frac{L_m}{L_s}\phi_s$ (13c)

The stator active and reactive power in (7) is expressed as,

$$P_s = -v_s\frac{L_m}{L_s}i_{qr} \quad (14a)$$

$$Q_s = v_s\frac{\phi_s}{L_s} - v_s\frac{L_m}{L_s}i_{dr} \quad (14b)$$

D. Statement problem

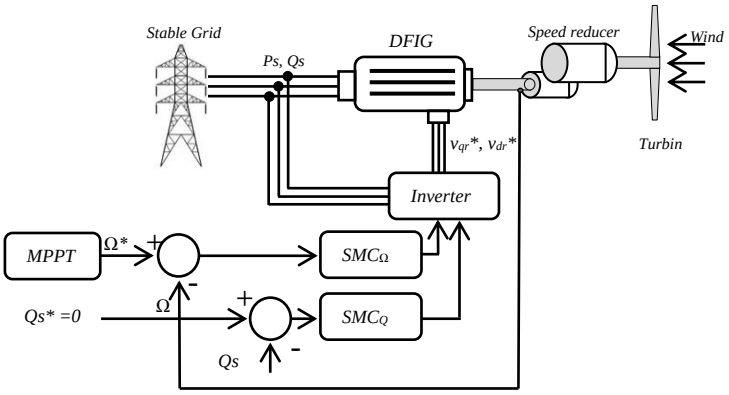

Figure-3. Wind turbine system controller.

As it's shown above in Figure-3, the control purpose is to introduce a novel strategy, which regroups an MPPT algorithm and a robust controller in order to maximize the wind turbine output power under external disturbances, fast wind change and unknown dynamics of WT.

3. MPPT ALGORITHM

The maximization of the mechanical input power does not always imply the maximization of the electrical output power [8] because of the variation of the DFIG yield under angular speed change, so the IPC algorithms will not be a relevant choice for our objective study.

Therefore, we limit ourselves to the DPC algorithms, and we chose the HCS algorithm to elaborate the present study to control DFIG, for its simplicity and its fast convergence time, instead of the INC and the ORB, which can be used only for wind turbines with AC/DC converters.

In the HCS algorithm, the wind turbine output power is directly controlled and optimized. It allows to reach the MPP at a given wind speed [4],[7], by locating the side of the MPP in the theoretical power curve, and force the generator, through a rotor side inverter, to reach it.

To achieve this goal, the inverter in rotor side, disturbs the output control variable, with some step value and measures the output power until the MPP [4], [7] is reached. However, and during rapid wind changes, the algorithm fails to locate the right side of the MPP.

To overcome this failure, the modified HCS algorithm has been proposed in [4],[8]. The variable step size and the direction of the next perturbation are calculated by observing the distance between the generator speed at the operating point and its corresponding in the optimal power curve [4], [8],[9],[10]at the operating power Figure-7.

In the modified HCS, there are three steps to track the MPP [4], [8] as follow:

Mode 0: Searches for a K_{opt} value with the aim to track peak point through HCS method.

Mode 1: Keeps the system at detected MPP for the constant wind speed (V_m).

Mode 2: In case of variable wind speed, the algorithm updates the value of K_{opt}, in the case of its change by climatic conditions [4], [8].

The HCS algorithm integrated with fixed and adaptive step size [4], [52], [53] performs the tracking of the MPP on the net power curve by incrementing or decrementing the speed reference (Ω_{ref}), with fixed value ($\Delta\Omega_{\text{fixed}}$) and adaptive value ($\Delta\Omega_{\text{adp}}$) respectively as it's shown in Figure-4 and Figure-5.

The algorithm starts with a fixed step($\Delta\Omega_{\text{fixed}}$) until the output power becomes negative, and then runs with$\Delta\Omega_{\text{adp}}$.

The adaptive step decrease around the MPP, therefore reducing the oscillations around it [4], [54], [55], [56], the flowchart in Figure-6, shows the three operation modes [4], [8].

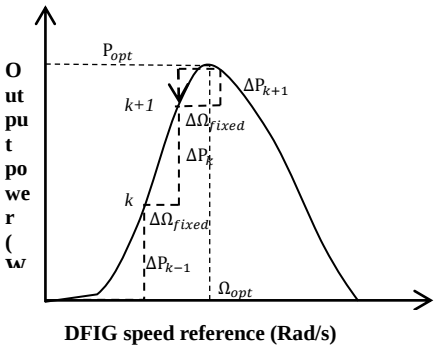

Figure-4. HCS control principle with fixed step.

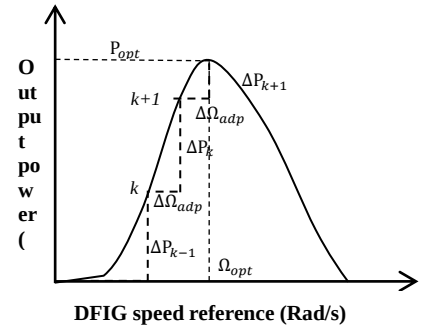

Figure-5. HCS control principle with adaptive step.

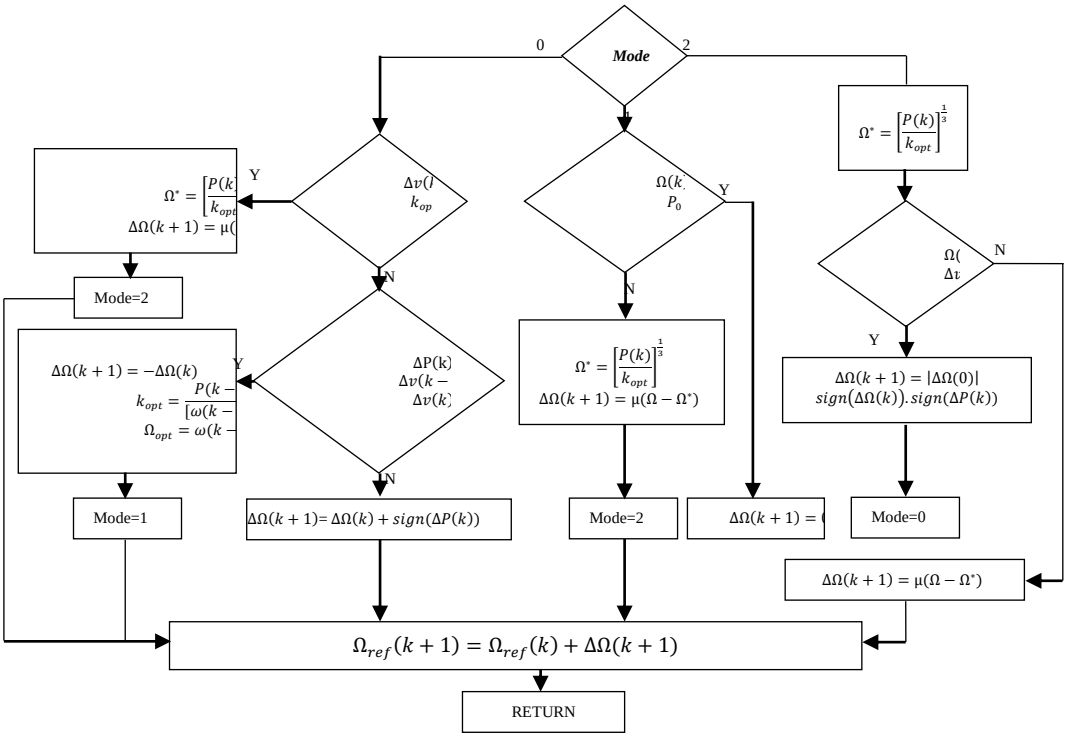

Figure-6. Modified HCS flowchart.

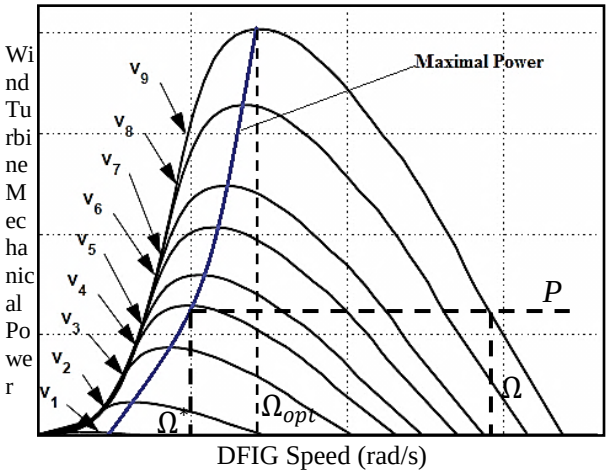

Figure-7. Adaptive tracking in mode 2 with variable step size.

The accuracy and the efficiency of the proposed algorithm [8] depend on the performance of the controller used, thus the significant inertia of wind turbine also influences the effectiveness of this algorithm.

Indeed, this algorithm introduces an improvement of classical HCS algorithms, which use a variable step to avoid the oscillations around the MPP, and the distance between the operating speed and its corresponding atthe optimal curve in the operating power Figure-7,to resolve the perturbation direction problem [8], this improvement requires a very fast system feedback under fast wind changes, and the speed set point should be achieved very fast and accurately. To this end, a robust controller based on sliding mode has been applied to control DFIG under various wind change.

The next section, details the different steps of controller law building, and a compared simulation has been performed to show the benefit of the proposed strategy as it shown in figure below.

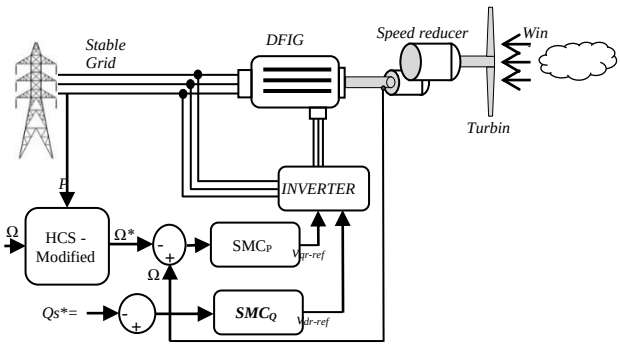

Figure-8. HCS MPPT algorithm with HOSM controller.

4. SLIDING MODE CONTROLLER

To design a sliding mode controller, there are three steps [50]:

a) Choosing a sliding surface,
b) Define the convergence conditions and
c) Design a stabilizing control law.

A. Sliding surface

The sliding surface S defines the desired dynamic behaviour of the system and the error convergence. The sliding surface is given by the following equation [50]:

$$S(x) = (\frac{\delta}{\delta t} + \lambda)^{n-1} e(x) \quad (15)$$

Where, λ is a strictly positive constant and n is the smallest positive integer to ensure controllability such that $\frac{d\dot{s}}{dt} \neq 0$
The variable e(x) is the error.

B. Convergence condition

Two conditions must be satisfied for the system to converge to the sliding surface: the reaching condition and the sliding condition. Consider a positive scalar function V (x) >0. The control law has to force the decrease of this function to make the sliding surface attractive and invariant [50]. Choosing

$$V(x) = \frac{1}{2} S(x)^2 \quad (16)$$

Taking the time derivative of *V(x)* results into the following condition,$\dot{V}(x) < 0$, i.e., $S(x).\dot{S}(x) < 0$.

C. Stabilizing control law

This condition is used to determine appropriate control laws that bring controlled variables to their respective sliding surface and keep them on it until the equilibrium point is reached.

The DFIG dynamic equations (3) and (13) can be written as,

$$J\frac{d\Omega}{dt} = C_t + P\frac{L_m}{L_s}\phi_s i_{qr} - \Omega.f \quad (17a)$$

$$\frac{di_{qr}}{dt} = \frac{1}{\sigma}(v_{qr} - R_r.i_{qr} - \omega_r.\sigma.i_{dr} - g\omega_r) \quad (17b)$$

$$\frac{di_{dr}}{dt} = \frac{1}{\sigma}(v_{dr} - R_r.i_{dr} + \omega_r\sigma.i_{qr}) \quad (17c)$$

Therefore, define the speed tracking sliding variable as,

$$S = \Omega - \Omega^* \quad (18)$$

Where, Ω*is the reference speed. Taking the derivative of *S*and substituting $\frac{d\Omega}{dt}$from (17a) yields,

$$\frac{dS(\Omega)}{dt} = \frac{1}{J}\left(C_t + P\frac{L_m}{L_s}\phi_s i_{qr} - \Omega.f\right) - \frac{d\Omega^*}{dt} \quad (19a)$$

$$\frac{d\dot{S}(\Omega)}{dt} = \frac{1}{J}\left(\dot{C}_t + P\frac{L_m}{L_s}\phi_s \frac{di_{qr}}{dt} - \dot{\Omega}.f\right) - \frac{d\dot{\Omega}^*}{dt} \quad (19b)$$

Substituting$\dot{\iota_{qr}}$from (17b) into (19b) leads to,

$$\frac{d\dot{S}(\Omega)}{dt} = \frac{1}{J}\left(\dot{C}_t + P\frac{L_m}{L_s}\phi_s(\frac{1}{\sigma}(\boldsymbol{v_{qr}} - R_r.i_{qr} - \omega_r.\sigma.i_{dr} - g\omega_r)) - \dot{\Omega}.f\right) - \frac{d\dot{\Omega}^*}{dt} \quad (20)$$

Where, v_{rq} is the control variable law of the wind turbine.

D. High order sliding *mode (*HOSM) controller design

The system (20), is a relative degree equals 2, compared with the sliding surface S(Ω), In [35],[36] the authors have proposed the HOSM controller, in order to control nonlinear systems, in this case the DFIG, and to reduce the chattering phenomenon, by introducing the twisting algorithm, whose control law expression is given by:

$$v_{qr} = -K(sign(S) + \beta.sign(\dot{S})) \quad (21)$$

Where,

sign(.) : function that returns the sign of its argument
β : positive constant and$0.5 \leq \beta < 1$.
K : constant controller gain.

Several methods, to define these parameters are proposed in the literature. In [35],[36]the authors have proposed sufficient conditions to define its, as described below:

The equation system (20) can be transformed as follow:

$$\ddot{S}(\Omega) = \psi(.) + \varphi(.)V_{rq} \quad (22a)$$

With:

$$\psi(.) = \frac{1}{J}\left(\dot{C}_t + P\frac{L_m}{L_s}\phi_s(\frac{1}{\sigma}(-R_r.i_{qr} - \omega_r.\sigma.i_{dr} - g\omega_r)) - \dot{\Omega}.f\right) - \frac{d\dot{\Omega}^*}{dt} \quad (22b)$$

And $\varphi(.) = P\frac{L_m}{J.L_s.\sigma}\phi_s$ (22c)

Are bounded functions.

ConsiderK_M, K_m, C positive constants, which satisfy:

$$0 < K_m \leq \varphi \leq K_M \; ; |\psi| < C \quad (23)$$

The sufficient conditions [35], [36],for the convergence of S and $\dot{S}$ to zero (sliding mode established)and Ω *to* $\Omega^*$are:

$$K_m.K(1+\beta) > C \quad (24a)$$

$$K_m.K(1+\beta) - C > K_M(1-\beta) + C \quad (24b)$$

These conditions are the minimum requirements for K to ensure the convergence of the twisting algorithm to the second order sliding mode. In the case of unknown bounds ofK_M, K_m, C, the value of K is overestimated which yields to chattering phenomenon.

To attenuate the chattering effect, it was proposed in [40], [41],[42] a novel strategy to adapt the controller gain. Thus, the controller law is defined as:

$$v_{qr} = -K(t)(sign(S) + \beta.sign(\dot{S})) \quad (25)$$

With$K(t)$is a time varying gain.

The idea is to increase the gain K, until the second order sliding mode is established. Then K is gradually reduced until the sliding mode is lost [40], [41], [42].

Introduce a criterion for the detection of the second order sliding mode with respect to sliding variable S. Consider a natural number N and some μ>0 and define [40], [41],[42]:

$$\alpha(t) = \begin{cases} 1 \text{ if } \forall\, t_j \in [t - N\tau, t]: \ |S(t_j)| \le \mu K(t_j)\tau^2 \\ -1 \text{ if } \exists\, t_j \in [t - N\tau, t]: \ |S(t_j)| > \mu K(t_j) \end{cases} \quad (26)$$

Withτ the sampling time, t_j the sampling instants. The 2^{nd} order sliding mode is established if $\alpha = 1$[40], [41],[42].

Introduce some constants,K_1,K_2such that

$$K_1 > K_2 > 0 \quad (27)$$

The law adaptation is given by [40], [41],[42]:

$$\dot{K}(t) = \begin{cases} -\alpha\lambda K \ \text{ if } K > K_1 \\ -\alpha\lambda_m \text{if} K_2 < K \le K_1; \ K(0) > K_2 \\ \lambda_m \text{ if } K < K_2 \end{cases} \quad (28)$$

Withλ_m,λpositive adaptation parameters. Thus, to control law (25) with time varying gain under the adaptation law (26)-(28), a second order sliding mode with respect to sliding variable S is established in finite time.

The algorithm stability and the convergence proof are detailed in[41],[42].

5. SIMULATION RESULTS AND DISCUSSIONS

A. Setup

To demonstrate the performance of the proposed approach, a computer simulation is carried out on the wind turbine model described in section II. Table-1 summarizes the system's parameters along with their respective values. HOSM controller coefficients are set toβ=0.9,K_1=100,K_2=1,λ_m=500, λ=500. The sampling frequency is set to 10 KHz.

PID controller parameters are set to: K=1000; Td=0.5s, Ti=0.5s and N=100;

HCS algorithm parameters are set to: μ=0.01, ΔΩ=1 rad/s.

Table-1. System's parameters.

Parameter	Value
Turbine's diameter (m)	d=45
Turbine's inertia (kg·m2)	Jt=16e^5
Air density (kg·m3)	ρ=1,2
Gear reduction ratio	r=100
Generator's inertia (kg·m2)	Jm=114
Generator's frequency (Hz)	F=50
Generator's q-axis stator voltage (V)	V=690
Generator's stator resistance(Ω)	Rs=0,00297
Generator's rotor resistance(Ω)	Rr=0,00382
Generator's stator inductance (H)	Ls=0,121
Generator's rotor inductance (H)	Lr=0,0573
Generator's cyclic inductance (H	Lm=0,031
Dispersion coefficient	σ=0,86

B. RESULTS AND DISCUSSIONS

A computer simulation is performed using Matlab/ SIMULINK to show the effectiveness of the proposed control strategy.

This simulation is based on two wind speed profiles as it shown in Figure-9and Figure-10.

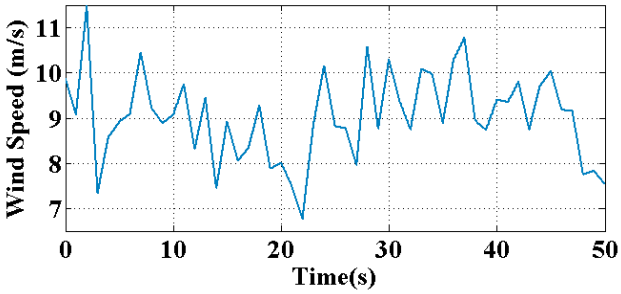

Figure-9. Wind speed in m/s versus time (sec): Fast change.

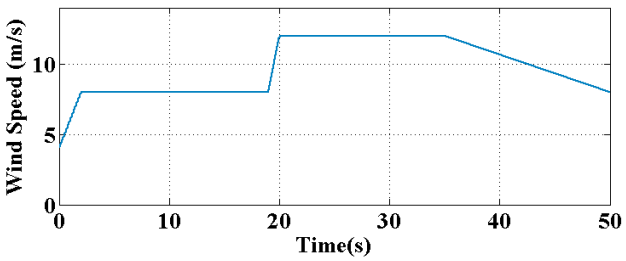

Figure-10. Wind speed in m/s versus time (sec): moderate change.

The modified HCS has the main advantage of correcting the problems encountered with the classical HCS. To show these problems a computer simulation, at the same step ($\Delta\Omega_{fixed} = 1\, rad/s$), between classical and

modified HCS, was carried out using the wind speed profile Figure-10.

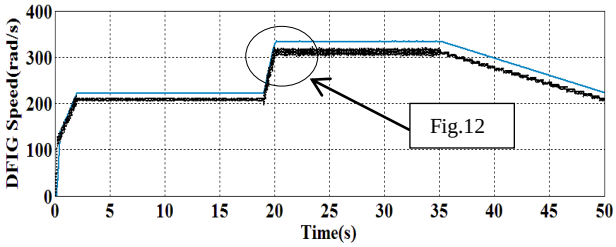

Figure-11. DFIG speed versus time (sec) in moderate change wind, Bleu: Adaptive step size HCS. Black: Fixed step size HCS.

The Figure-11shows the main failure of the HCS with fixed step size, it's the oscillations around the MPP, as well as the false MPP location, when there is a change in the wind speed.

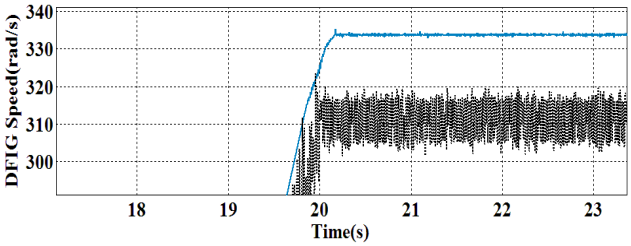

Figure-12. DFIG optimal speed around the MPP, Bleu: adaptive step size HCS; Black: Fixed step size HCS.

The unpredictable wind speed is considered such as perturbation source for the system. The proposed approach allows the system to track the MPP under fast wind change as it's shown in Figure-13 bellow.

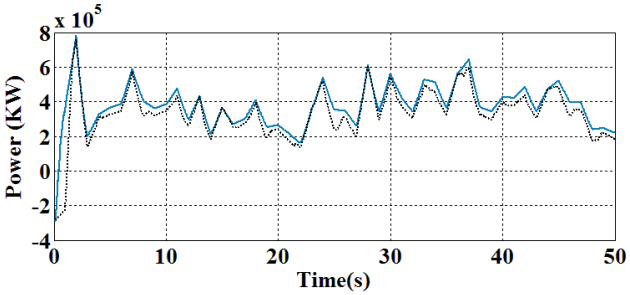

Figure-13. Optimal WT power versus time, in bleu the power tracked with robust controller, Black: with PID controller.

In the figure above, we can see that the power generated by the wind turbine using a sliding mode controller is greater than that using the PID, this shows that the efficiency and the accuracy of the MPPT algorithm depend strongly to the controllerbehavior.

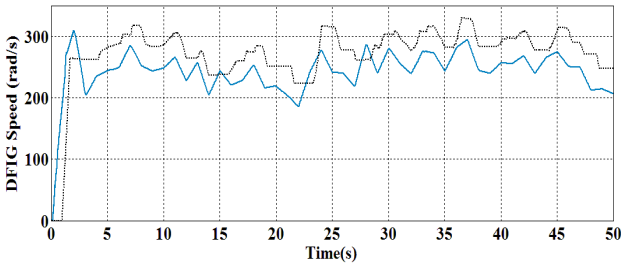

Figure-14. DFIG Angular speed detail versus time (sec): Bleu with HOSM controller, Black: with PID controller.

In this Figure, we can notice that the generator speed using a PID controller is more significant than that using the HOSM controller. This is due to the PID's low ability to recover quickly the optimal trajectory generated by the MPPT, under wind speed rapid change.

In the HOSM controller with adaptive gain as it described in section IV, the controller increase its gain value (or decrease it as required) in order to follow the set point quickly, and reject perturbations.

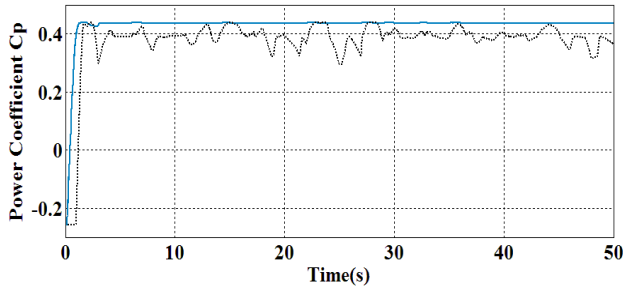

Figure-15. Power coefficient Cp, Bleu: with HOSM controller, Black with PID controller

This figure above shows that the use of a HOSM controller makes it possible to maintain the coefficient Cp at a maximum value despite the rapid change of the wind speed. In the other hand, the PID regulator (black curve) is very sensitive to rapid changes in wind speed, which causes a decrease in MPPT efficiency.

6. CONCLUSIONS

In this paper, a novel control strategy is introduced for doubly fed induction generator (DFIG), used in wind turbines. This strategy is based on HCS modified MPPT algorithm with a robust controller based on high order sliding mode using adaptive twisting algorithm.

The modified HCS makes it possible to correct the problems presented in the classical HCS, namely the oscillations around the MPP caused by the choice of a fixed perturbation step, and the problem of the perturbation direction when the change in the power is due to a change in wind speed.

The performance of this algorithm depends strongly on the controller used to control the wind turbine speed. For this we have introduced a controller based on

sliding mode to benefit from the advantages of the MPPT algorithm.

The major disadvantage of sliding mode controllers is the chattering phenomenon and the gain controller determining, these two problems have been corrected by the introduction of higher order sliding mode and the use of an adaptive gain algorithm respectively.

The adaptive gain controller is performed by using a twisting algorithm, which has as main advantage to keep the robustness of sliding mode controllers, reduce the chattering effect and adapt its parameters as required, which not allowed by classical algorithms with fixed parameters.

Thus, the proposed technique achieves high accuracy despite inherent wind turbine nonlinearities and unpredictable wind speed fluctuations.

Results show high accuracy and the fast convergence under various wind speed operating conditions. Thus, the performance of the proposed strategy is a key to achieve the high efficiency needed for high performance wind turbines.

A wind turbine model is used to validate the proposed approach.

REFERENCES

[1] Rik W. De Doncker. 2002. Doubly fed induction generator systems for wind turbines. IEEE Industry Applications Magazine.

[2] L. Holdsworth, W. Xue Guang, N.J.Janaka, B. Ekanayake. 2003. Dynamic Modeling of Doubly Fed Induction Generator Wind Turbines. IEEE transactions on power systems. 18(2).

[3] M. Enamul. Haque, M. Negnevitsky & K. M. Muttaqi.2010.A novel control strategy for a variable-speed wind turbine with a permanent magnet synchronous generator. IEEE Transactions on Industry Applications. 46(1): 331-339.

[4] D. Kumar, K. Chatterjee. 2016. A review of conventional and advanced MPPT algorithms for wind energy systems. Renewable and Sustainable Energy Reviews. 55(2016): 957-970.

[5] M. Nasiri, J. Milimonfared, S.H. Fathi. 2014. Modeling, analysis and comparison of TSR and OTC methods for MPPT and power smoothing in permanent magnet synchronous generator-based wind turbines. Energy Conversion and Management. 86: 892-900.

[6] Lucy Y. Pao and Kathryn E. Johnson. 2009. A Tutorial on the Dynamics and Control of Wind Turbines and Wind Farms. American Control Conference.

[7] M.A. Abdullah, A.H.M. Yatim, C.W. Tan, R. Saidur. 2012. A review of maximum power point tracking algorithms for wind energy systems. Renewable and Sustainable Energy Reviews. 16: 3220-3227.

[8] S. M Raza Kazmi, H. Goto. 2011. A Novel Algorithm for Fast and Efficient Speed-Sensorless Maximum Power Point Tracking in Wind Energy Conversion Systems. IEEE transactions on industrial electronics. 58(1).

[9] R. Ahmed, A. Namaane N. K. M'Sirdi. 2013. Improvement in Perturb and Observe Method Using State Flow Approach. The Mediterranean Green Energy Forum, MGEF-13.

[10] N. Femia, G. Petrone, G. Spagnuolo, M.Vitelli. 2005. Optimization of Perturb and Observe Maximum Power Point Tracking Method. IEEE transactions on power electronics. 20(4).

[11] David A. Torrey. 2002. Switched Reluctance Generators and Their Control. IEEE transactions on industrial electronics. 49(1).

[12] J. Prasanth Rama, N. Rajasekara, M. Miyatake. 2017. Design and overview of maximum power point tracking techniques in wind and solar photovoltaic systems: A review. Renewable and Sustainable Energy Reviews. 73: 1138-1159.

[13] S. Zahra Mirbagheri, Saad Mekhilef, S. Mohsen Mirhassani. 2013. MPPT with Inc. Cond method using conventional interleaved boost converter. Mediterranean Green Energy Forum (MGEF-13).

[14] B. Bendib, H. Belmili, F.Krim. 2015. A survey of the most used MPPT methods: Conventional and advanced algorithms applied for photovoltaic systems. Renewable and Sustainable Energy Reviews. 45-637-648.

[15] S. H. Hosseini, A. Farakhor, S. K. Haghighian. 2013. Novel Algorithm of Maximum Power Point Tracking (MPPT) for Variable Speed PMSG Wind Generation Systems through Model Predictive Control Electrical and Electronics Engineering (ELECO), 8th International Conference.

[16] K. Nan Yu, C. Kang Liao. 2015. Applying novel fractional order incremental conductance algorithm to

design and study the maximum power tracking of small wind power systems. Journal of Applied Research and Technology. 13: 238-244.

[17] C. Carrillo, A. F. Obando Montaño, J. Cidràs, E.D. Dorado. 2013. Review of power curve modelling for wind turbines. Renewable and Sustainable Energy Reviews. 21: 572-581.

[18] M.A. Abdullah, A.H.M. Yatim, C.W. Tan. 2014. An online Optimum-Relation-Based Maximum Power Point Tracking Algorithm for Wind Energy Conversion System. Australasian Universities Power Engineering Conference, AUPEC.

[19] A. G Abo-Khalil, D-C Lee, J.K Seok. 2004. Variable Speed Wind Power Generation System Based on Fuzzy Logic Control for Maximum Output Power Tracking.35th Annual IEEE Power Electronics Specialists Conference.

[20] M. Pucci, M. Cirrincione. 2011. Neural MPPT Control of Wind Generators with Induction Machines without Speed Sensors. IEEE Transactions on Industrial Electronics.

[21] A. Oukaour, H.Gualous. 2014. Maximum Power Point Tracking of Wind Turbines with Neural Networks and Genetic Algorithms. Conference: iecon'14, At Dallas.

[22] A.J. Saavedra-Montes; E. Arango. 2012. Maximum power point tracking in wind farms by means of a multivariable algorithm. Engineering Applications (WEA).

[23] D. Telford, M. W. Dunnigan, B.W. Williams. 2003. Online Identification of Induction Machine Electrical Parameters for Vector Control Loop Tuning.IEEE transactions on industrial electronics. 50(2).

[24] X. del Toro Garcia, A. Arias, M.G. Jayne, P.A. Witting. 2008. Direct Torque Control of Induction Motors Utilizing Three-Level Voltage Source Inverters.IEEE transactions on industrial electronics. 55(2).

[25] J. Beerten, Jan Verveckken, J. Driesen. 2010. Predictive Direct Torque Control for Flux and Torque Ripple Reduction. IEEE transaction on industrial electronic. 57(1): 404-412.

[26] K. Basu, J. S. Siva Prasad, G. Narayanan, H. K. Krishnamurthy, R Ayyanar. 2010. Reduction of Torque Ripple in Induction Motor Drives Using an Advanced Hybrid PWM Technique. IEEE transactions on industrial electronics. 57(6).

[27] M. A. Fnaiech, F. Betin, G. A Capolino, F. Fnaiech. 2010. Fuzzy Logic and Sliding-Mode Controls Applied to Six-Phase Induction Machine With Open Phases. IEEE transactions on industrial electronics. 57(1).

[28] H. Chaoui, P. Sicard, W. Gueaieb. 2009. ANN-Based Adaptive Control of Robotic Manipulators with Friction and Joint Elasticity. IEEE transactions on industrial electronics. 56(8).

[29] H. Chaoui; P. Sicard. 2010. Adaptive Fuzzy Logic Motion and Posture Control of Inverted Pendulums with Unstructured Uncertainties. 6th annual IEEE Conference on Automation Science and Engineering; Toronto, Ontario, Canada.

[30] T. O. Kowalska, M. Dybkowski, K. Szabat. 2010. Adaptive Sliding-Mode Neuro-Fuzzy Control of the Two-Mass Induction Motor Drive without Mechanical Sensors. IEEE transactions on industrial electronics. 57(2).

[31] C. M. Lin, C. F. Hsu. 2005. Recurrent-Neural-Network-Based Adaptive-Backstepping Control for Induction Servomotors. IEEE transactions on industrial electronics. 52(6).

[32] M. Wlas, Z. Krzemin´ski, J. Guzin´ski, H. Abu-Rub, H. A. Toliyat. 2005 .Artificial-Neural-Network-Based Sensorless Nonlinear Control of Induction Motors .IEEE transactions on energy conversion. 20(3).

[33] Utkin, V.I. 1977. Variable structure systems with sliding modes. IEEE Transactions on Automatic Control. 26(2): 212-222.

[34] Amimeur H, Abdessemed R, Aouzellag D, Merabet E, Hamoudi F. 2010. A sliding mode control associated to the field-oriented control of dual-stator induction motor drives. J Electr Eng.

[35] A. Levant. 1993. Sliding order and sliding accuracy in sliding mode control. International Journal of Control. 58(6):1247-1263.

[36] L. Fridman, A Levant. 1999. High Order Sliding Mode, CHAPTER 3 p. 30.

[37] H. Amimeur, D. Aouzellag, R. Abdessemed, K. Ghedamsi. 2012. Sliding mode control of a dual-stator

induction generator for wind energy conversion systems. International Journal of Electrical Power & Energy Systems.

[38] B. Beltran, T. Ahmed-Ali, M. Benbouzid. 2009. High-Order Sliding-Mode Control of Variable-Speed Wind Turbines. IEEE transactions on industrial electronics. 56(9).

[39] S. Ben Elghali, M. Benbouzid, T. Ahmed-Ali, J. Charpentier. 2010. High-Order Sliding Mode Control of a Marine Current Turbine Driven Doubly-Fed Induction Generator. 402 IEEE journal of oceanic engineering. 35(2).

[40] M. Hafiane J. Sabor, M. Taleb, H. Gualous, H. Chaoui. 2015. Adaptive Second Order Sliding Mode Speed Control of Doubly Fed Induction Generator Wind Turbines. Renewable and Sustainable Energy Conference (IRSEC) 3rd International.

[41] M. Taleb, A. Levant, F. Plestan. 2013. Pneumatic actuator control: Solution based on adaptive twisting and experimentation. Control Engineering Practice 21-727-736.

[42] M. Taleb, A. Levant, F. Plestan. 2012. Twisting algorithm adaptation for control of electro-pneumatic actuators. 12th IEEE Workshop on Variable Structure Systems, VSS'12.

[43] Y. Shtessel, M. Taleb, F. Plestan.2012. A novel adaptive-gain supertwisting sliding mode controller: Methodology and application. Automatica. 48- 759-769.

[44] F. Plestan, A. Chriette. 2012. A robust controller based on adaptive super-twisting algorithm for a3DOF Helicopter.51st IEEE Conference on Decision and Control.

[45] B. Beltran, T. Ahmed-Ali, M. El Hachemi Benbouzid. 2008. Sliding Mode Power Control of Variable-Speed Wind Energy Conversion Systems. IEEE transactions on energy conversion. 23(2).

[46] S. Ben Elghali. 2010. Modelling and control of a marine current turbine-driven doubly fed induction generator. IET Renewable Power Generation.

[47] E. S. Abdin; W. Xu. Control. 2000. Design and Dynamic Performance Analysis of a Wind Turbine-Induction Generator Unit. IEEE Transactions on Energy Conversion. 15: 91-96.

[48] S. M. Barakati. 2008. Modeling and controller design of a wind energy conversion system including a matrix converter. Ph.D. dissertation, Dept. Electr. Comp. Eng., Univ. Waterloo, Waterloo, ON, Canada.

[49] G. Abad, M. A. Rodrìguez, J. Poza and J. M. Canales.2010. Direct Torque Control for Doubly Fed Induction Machine-Based Wind Turbines Under Voltage Dips and Without Crowbar Protection. IEEE transactions on energy conversion. 25(2).

[50] R. Pradhan, B. Subudhi. 2016. Double Integral Sliding Mode MPPT Control of a Photovoltaic System. IEEE transactions on control systems technology. 24(1).

[51] M. Benbouzid, B. Beltran, Y. Amirat, G. Yao, J. Han, H. Mangel. 2013. High-Order Sliding Mode Control for DFIG-Based Wind Turbine Fault Ride-Through. IEEE IECON 2013, Vienne: Austria.

[52] J. Yaoqin,Y.Zhongqing, C. Binggang. 2002. A new maximum power point tracking control scheme for wind generation. Int. Conf Power SystTechnol: 144-8.

[53] Z. M. Dalala, Z. U. Zahid, W. Yu, Y. Cho,J. S Lai. 2013. Design and Analysis of an MPPT Technique for Small-Scale Wind Energy Conversion Systems. IEEE transactions on energy conversion. 28(3).

[54] A. Harrag, S. Messalti. 2015. Variable step size modified P&O MPPT algorithm using GA-based hybrid offline/online PID controller. Renewable and Sustainable Energy Reviews. 49-1247–1260.

[55] T. Thiringer, J. Linders. 1993. Control by variable rotor speed of a fixed-pitch wind turbine operating in a wide speed range. IEEE Trans Energy Convers. 8:520-6.

[56] M Jinbo, G. C Junior, F. A. Farret, D. L. Hoss, M.C. Moreira. 2014. Fixed and adaptive step HCC algorithms for MPPT of the cylinders of magnus wind turbines.3rdRenew Power GenerConf: 1-6.